Kinetics and Mechanism of the Synthesis of a Novel Protein-Based Plastic Using Subcritical Water

ARTICLE *in* BIOTECHNOLOGY PROGRESS · MARCH 2008

Impact Factor: 2.15 · DOI: 10.1021/bp0702572 · Source: PubMed

2 AUTHORS, INCLUDING:

Hiroyuki Yoshida
Putra University, Malaysia
129 PUBLICATIONS **2,678** CITATIONS

Kinetics and Mechanism of the Synthesis of a Novel Protein-Based Plastic Using Subcritical Water

Wael Abdelmoez* and Hiroyuki Yoshida

Department of Chemical Engineering, Osaka Prefecture University, Osaka 599-8531, Japan

We investigated the intermolecular mechanism and kinetics of the synthesis of a novel biodegradable protein-based plastic from bovine serum albumin under subcritical water conditions using batch reactors. The reaction mechanism could be viewed as a chain reaction stabilized by the formation of intermolecular disulfide bonds. The kinetic analysis was based on non-steady-state kinetics using a theoretical model developed in one of our previous works. The activation energy and pre-exponential factor were found to be 7.2 kJ/mol and 0.9 s^{-1}, respectively. These low values signify that the reaction is relatively temperature-insensitive with some diffusion limitation.

Introduction

The key properties of water that influence many of the most important interactions are the ion product (the product of the hydrogen ion concentration and the hydroxyl ion concentration) and dielectric constant (which reflects the polarity and solvent ability of water). Increasing the ion product value increases the hydrogen ion concentration. Therefore, under high ion product values water possesses the effect of an acid catalyst (*1*). Also, a decrease of the dielectric constant decreases the water polarity. Both the ion product value and dielectric constant of water can be controlled through the temperature and pressure of the water (*2*, *3*). On heating beyond the critical point (temperature > 374 °C, pressure >22.1 MPa), the supercritical water shows extremely active and corrosive performance. However, water within the critical point under enough pressure to maintain the liquid state, which is called subcritical water (hereafter called sub-CW), can perform very selective extractions and synthetic processes (*4*−*6*). Such mild conditions of sub-CW has attracted many researchers. Different organic pollutants and waste have been treated utilizing sub-CW including decomposition of hazardous organic (*7*), municipal sewage sludge (*8*), and marine waste (*6*). In our laboratory, it was shown that sub-CW under an inert atmosphere in the absence of oxygen or oxidant can perform very selective extractions of polar (at lower temperatures), moderately polar, and nonpolar (at higher temperatures) substances. Moreover, it activated many hydrolysis reactions without the need of additional catalysts (*9*). On the basis of this idea, Yoshida et al. showed that a relatively large amount of oil, organic acids, and amino acids could be extracted from fish, squid entrails, and meat wastes by the sub-CW technology (*9*−*14*). Furthermore, many useful products were extracted from wood wastes such as construction scraps and thinning materials using the sub-CW technology (*15*). An overview for the applications of the sub-CW technology in the field of waste reuse, recycle, and treatment is provided in ref 16.

Serum albumin represents the most abundant protein in blood serum, with a typical concentration of 50 g/L. The word albumin is also used to describe a protein or a group of proteins defined by their solubility in water, such as those found in the albumin fraction of wheat and serum albumin of proteins in whey-milk. Typically, bovine serum albumin (BSA) is a monomeric highly water-soluble protein with a molecular weight of 66 kD. In our previous work (*17*) using BSA, we succeeded in synthesizing a novel biodegradable plastic BSA (PBSA). The synthesis processes was carried out using sub-CW in a batch reactor within a very short reaction time (1 min) at 523 K. The polymerization of the BSA was catalyzed under the sub-CW condition without any additives. In this way, we provided a new method for blood waste treatment and at the same time a new synthesis method for a novel biodegradable plastic. Such a plastic could have applications in the biodegradable plastic field and the medical clinic as a new implantation material. Reaction conditions involved temperatures of 473−573 K, pressure of 1.55−8.59 MPa, and a reaction time of 30−60 s using 160 g/L BSA as an initial BSA concentration. Results showed that after 30 s all BSA molecules were completely transformed into water-insoluble solids, which showed many plastic properties and represented the plastic BSA. Both optimum temperature and time of the reaction under the sub-CW condition were found to be in the range of 523−548 K and 30−60 s, respectively.

For more understanding and better reactor design for the synthesis of the PBSA, both the reaction mechanism and rate equations governing the production of this useful material under the sub-CW condition should be clarified.

The synthesis procedures of the PBSA included the immersion of a stainless steel batch reactor containing a solution of BSA into a hot salt bath for a short reaction time. Then the reactor is quickly quenched in cold water to stop the reaction. On the basis of these procedures it is apparent that under such a short immersion time the temperature inside the reactor will not attain the salt bath temperature, and therefore the actual reaction temperature is lower than the temperature of the salt bath. Accordingly, during the synthesis period the temperature inside the batch reactor is continuously rising with time, and therefore the synthesis process was taking place very quickly under non-steady-state conditions. As a result, in another previous work we had to develop a new mathematical model for describing the kinetic behavior of fast reactions in batch reactors using sub-CW under non-steady-state conditions (*18*). It is important

* To whom correspondence should be addressed. Ph: +81-72-254-9301. Fax: +81-72-254-9911. Email: drengwael2003@yahoo.com.

10.1021/bp0702572 CCC: $40.75
Published on Web 02/06/2008

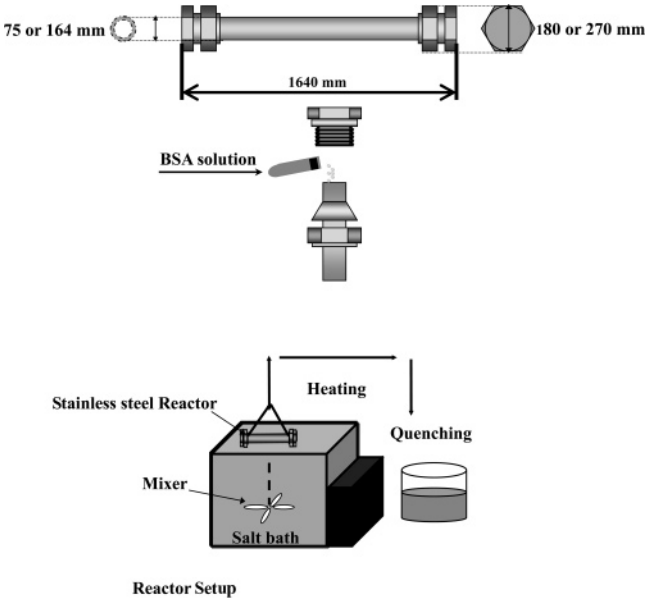

Figure 1. Reactor configuration and setup used for the PBSA synthesis using the sub-CW technology.

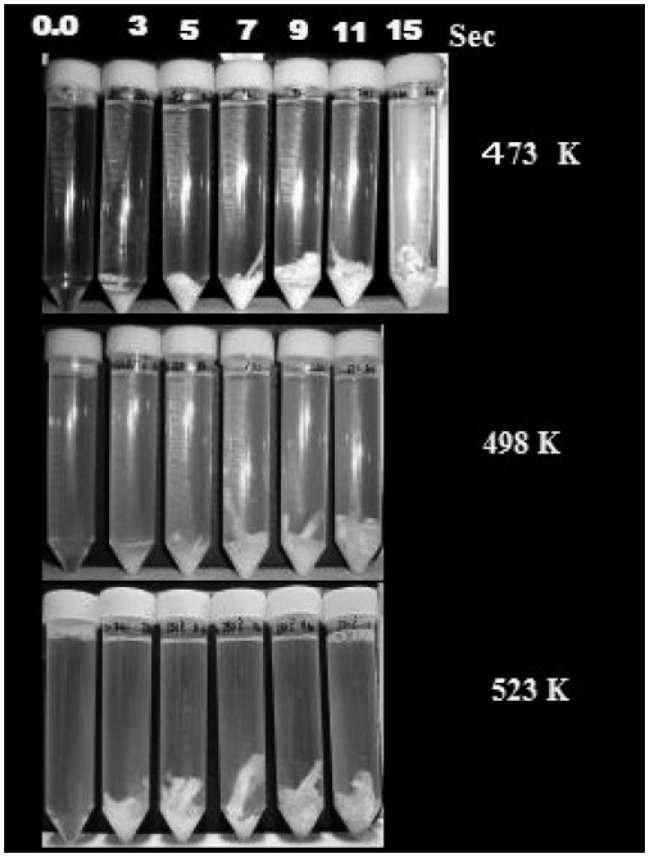

Figure 2. Photographs of the BSA reaction mixture before and after sub-CW reaction at 473, 498, and 523 K at different interval times.

to note here that the best reactor to follow the kinetics of such fast reactions could be the continuous flow type of reactor. However, the PBSA synthesis could not be investigated using a continuous reactor due to the plugging of the reactor tubes resulting from the rapid formation of the solid PBSA, which hindered the flow of both reactants and product.

In the present work we investigated the intermolecular mechanism and kinetics of the PBSA synthesis in batch reactors based on the theoretical models developed in our previous work (*18*). This work also represents the first step in the understanding of both the kinetics and mechanism of the water-soluble protein hydrolysis and decomposition under the sub-CW condition.

Materials and Methods

Materials. Pure BSA and other chemicals used in this study were purchased from Wako Pure Chemical Industries, Ltd. (Osaka, Japan). The BSA was found to be homogeneous by SDS−PAGE with 5% water content, and it was used as purchased without any further purification.

Experimental Procedures. ***Measuring Temperature Profiles inside the Batch Reactor.*** The synthesis reactions were carried out using relatively small and large reactors. Two different stainless steel pipes, SUS 316, i.d. 0.0075 m × 0.15 m (with a reactor volume of 9.0×10^{-6} m^3) and i.d. 0.0168 m × 0.15 m (with a reactor volume of 34×10^{-6} m^3), with Swadgelok caps were used as small and large reactors, respectively. The temperature profiles inside the small reactor were measured, and both heating and cooling rate constants were obtained according to the method described in our previous work (*18*).

Kinetics of the Synthesis Reaction of PBSA. The synthesis procedures were carried out according to the PBSA synthesis method described in our previous work (*17*).

The kinetic experiments were performed in the small reactor. The reactions were carried out at 473, 498, and 523 K. At a predetermined time the product of the reaction was recovered from the reactor, diluted to 50 mL with Milli-Q water, and filtrated through a Millipore membrane (2.2×10^{-7} m) to separate the solid PBSA from the liquid phase. The protein concentration in the filtrate was measured using a Shimadzu UV-2100 spectrophotometer (Shimadzu Co. Ltd., Kyoto, Japan) assuming $\epsilon = 0.55$ (g/L) $^{-1}$·cm^{-1} at 279 nm. The protein identification in the filtrate was performed by SDS−PAGE using an acrylamide concentration of 4% for stacking and 15% for resolving gels (*19*). The BSA band was identified using a standard molecular weight marker under identical electrophoretic conditions (*20*).

Intermolecular Bonds Involved in the PBSA Formation. To investigate the nature and type of bonds involved in the PBSA formations, we followed the strategy and experimental methods described by Robert and others (*21*) in their study concerning the moisture-induced aggregation of the BSA. Accordingly, the solubility of the powdered PBSA in different denaturants, including 6 M urea; 6 M guanidine hydrochloride; or a mixture of 6 M guanidine hydrochloride, 10 mM EDAT, and 0.2 M dithiothertol (DTT), were measured. In a 50-mL plastic test tube, 0.1 g of dried and powdered PBSA were mixed with the test solution containing one of the above-mentioned denaturants and stirred for 24 h. Then, the test tubes were centrifuged at 3,000 × *g* for 10 min at room temperature. The protein concentration in the filtrate was measured using a Shimadzu UV-2100 spectrophotometer (Shimadzu Co. Ltd., Kyoto) assuming $\epsilon = 0.55$ (g/L) $^{-1}$·cm^{-1} at 279 nm.

Aggregation of BSA under Atmospheric Pressure. Different test tubes were charged with 2.5 mL of a BSA solution with a concentration of 160 g/L and heated in a dry block bath (Toyo Seisakusho Kaisha Co. Ltd., Tokyo, Japan) with an average heating rate of 5 K/min under atmospheric pressure. The aggregation was observed in the temperature range of 298−363 K and recorded using a digital camera to detect the initiation of the aggregation process.

Electron Microscopy. A JEOL 6700F field emission scanning electron microscopic (SEM) (JEOL Inc., MA) was used to observe the microstructure of the prepared PBSA. Solid dry

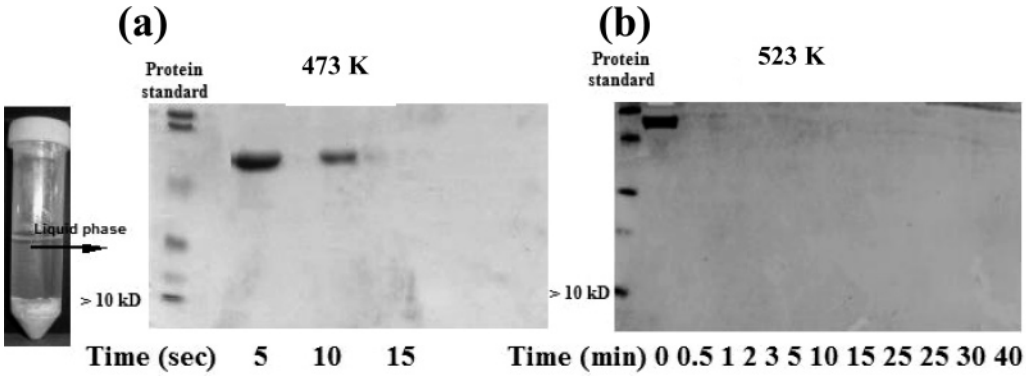

Figure 3. Electrophoresis patterns of the aqueous phase of the BSA reaction mixture after sub-CW reaction at 473 and 523 K at different interval times (minutes).

samples of the PBSA were prepared for the SEM according to the manufacture instruction.

Theory. Because the PBSA was synthesized in a short time (30−60 s) under non-steady-state conditions (*17*), it was necessary to explore the batch reactor system, which will be used in the kinetic study. Generally, batch reactors were characterized by heating and cooling periods. During the heating period the temperature continuously increased with increase in the reaction rate and vice versa for the cooling period. Accordingly, first we must determine equations describing the temperature profile inside the reactor during these periods as well as analyzing the kinetics involved in the synthesis process. In our previous work (*18*), we carried out a detailed study for simulating fast reactions under the sub-CW condition using the same batch reactor used in this study. The temperature profiles inside the reactor were investigated under different operating conditions. The most important parameters that may affect the temperature profile, including salt bath mixing speed, reactor shaking, reactant viscosity, and reactor contents, were investigated both experimentally and theoretically. Two different empirical equations were obtained to describe the temperature profiles during both heating and cooling stages. Using these equations, we developed a new mathematical model for describing the kinetic behavior of the fast reactions that take place under the sub-CW conditions. In that model, we assumed that the reaction proceeded under non-steady-state conditions and following a first-order kinetic. On the basis of the simulation results, we developed a new strategy for finding the correct values of the kinetic parameters such as activation energy and pre-exponential factor (sometimes called frequency factor). In this study, we used the same mathematical model and strategy developed in that previous work (*18*).

Results and Discussions

Intermolecular Mechanism. To investigate the kinetic and mechanism of the PBSA synthesis, the time courses of the BSA reactions under the sub-CW condition were studied at 473, 498, and 523 K during early stages of the synthesis in the period of 2−30 s. The rector configuration and set up used in this study are shown in Figure 1.

Figure 2 shows photographs of the reaction products at 473, 498, and 523 K for different reaction times compared to a photograph of the solution of the BSA before the reaction. As shown in the photos, as the temperature of the reaction and the reaction time increase, the amount of PBSA formed increases. To follow the intermolecular mechanism, we have to answer two important questions.

First, we questioned if the unconverted BSA at a very short reaction time is subjected to a fragmentation process before going to the polymerization step or if it maintains the same primary structure until it aggregates and polymerizes. The answer for such questions was given by measuring the protein existence and its status in the liquid phase after the reaction using SDS−PAGE electrophoresis. Figure 3a shows the electrophoresis patterns of the BSA reaction mixture in the liquid phase after sub-CW reactions at 473 K for 5, 10, 15, and 30 s, respectively, compared to reactions took place at 523 K at different reaction times in the range of 0.5−40 min. The results showed the appearance of the BSA band after reaction times of 5 and 10 s and its disappearance after 15 s reaction time. However, at 523 K, all of the water-soluble BSA molecules transferred into solid PBSA after 0.5 min reaction time (Figure 3b). Moreover, no protein bands were observed other than the BSA band. From these results it became clear that the BSA molecules did not fragment and directly aggregated and polymerized. This conclusion agrees with the results obtained in our previous work concerning the synthesis of the PBSA (*17*). It was proved that there were no amino acids produced within a reaction time of 2 min in the temperature ranges of 473−523 K.

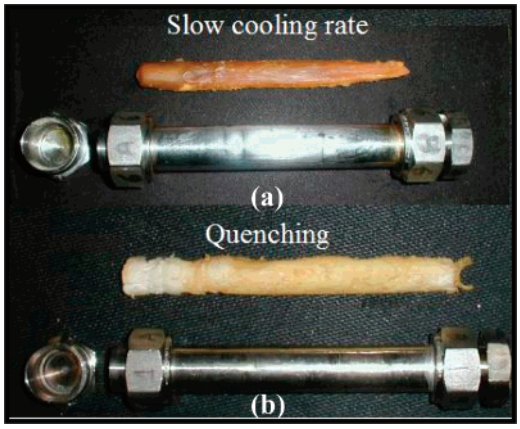

Figure 4. Photographs of the PBSA prepared using sub-CW at 523 K for 1-min reaction time either (a) air-cooled or (b) quickly quenched in cold water.

Second, we questioned weather the PBSA was formed as a result of the quenching step or the sub-CW reaction. To get an answer for this question, two batches of the PBSA synthesis were carried out under identical conditions at 523 K using the large reactors. After 1 min reaction time, one of the reactors was quickly quenched into a cold water to stop the reaction immediately, while the other was left to cool down slowly on the air without any quenching process (which took more than 30 min to reach 298 K). Figure 4 shows photographs of both cases. The results showed that in both cases the PBSA was

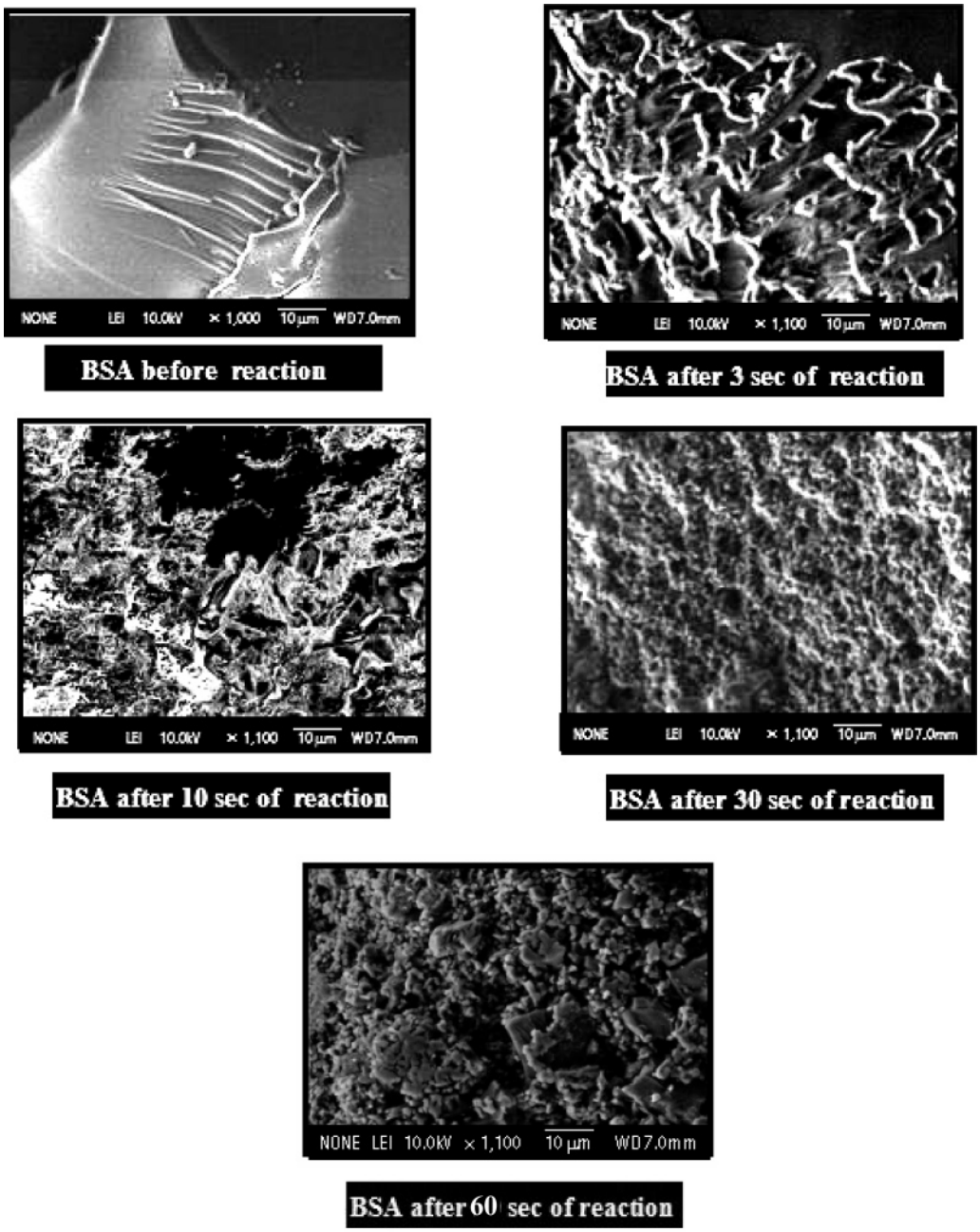

Figure 5. SEM micrograph of the native BSA and the formed PBSA after sub-CW reaction at 523 K for different interval times.

Table 1. Solubility of Powdered PBSA in Different Solutions

solution composition	solubility [%]
distilled water	0
6 M urea	5
6 M guanidine hydrochloride	7
6 M guanidine hydrochloride + 10 mM EDAT + 0.2 M dithiothertol	83

formed; however, in the case of slow cooling, the PBSA subjected to roasting and decomposing processes as indicated by the changing in color from bright yellow (for the sample prepared by quick quenching) to a brown one. Besides, the recovery of the PBSA decreased dramatically from 85% for quick water-quenched sample to 66% for the air-cooled sample. This lower recovery value was due to the weight loss of the PBSA during the hydrolysis and decomposition reactions. These results indicated that the aggregation and polymerization process took place as a result of the sub-CW reaction and not the quenching process.

To explore the structural changes of the PBSA during the early stages of the synthesis, EMS images were taken for dry PBSA samples prepared at short intervals. Figure 5 shows the micrographs from SEM of the native BSA compared to the solid formed after the sub-CW reaction at 523 K for different intervals. The micrograph of the native BSA showed a smooth surface structure and was easily differentiated from that polymerized under the sub-CW condition. After 3 s reaction time under the sub-CW conditions, BSA started to coagulate to form a thin-stranded interconnected network structure with less consistent structure. After 10 s, the BSA aggregated more, having less voids and rather strong structure. However, after 30 s, the BSA polymerized, forming a clear clustering structure. After 60 s reaction, these clusters gathered to form bulks of clusters having a structural differentiation with different size.

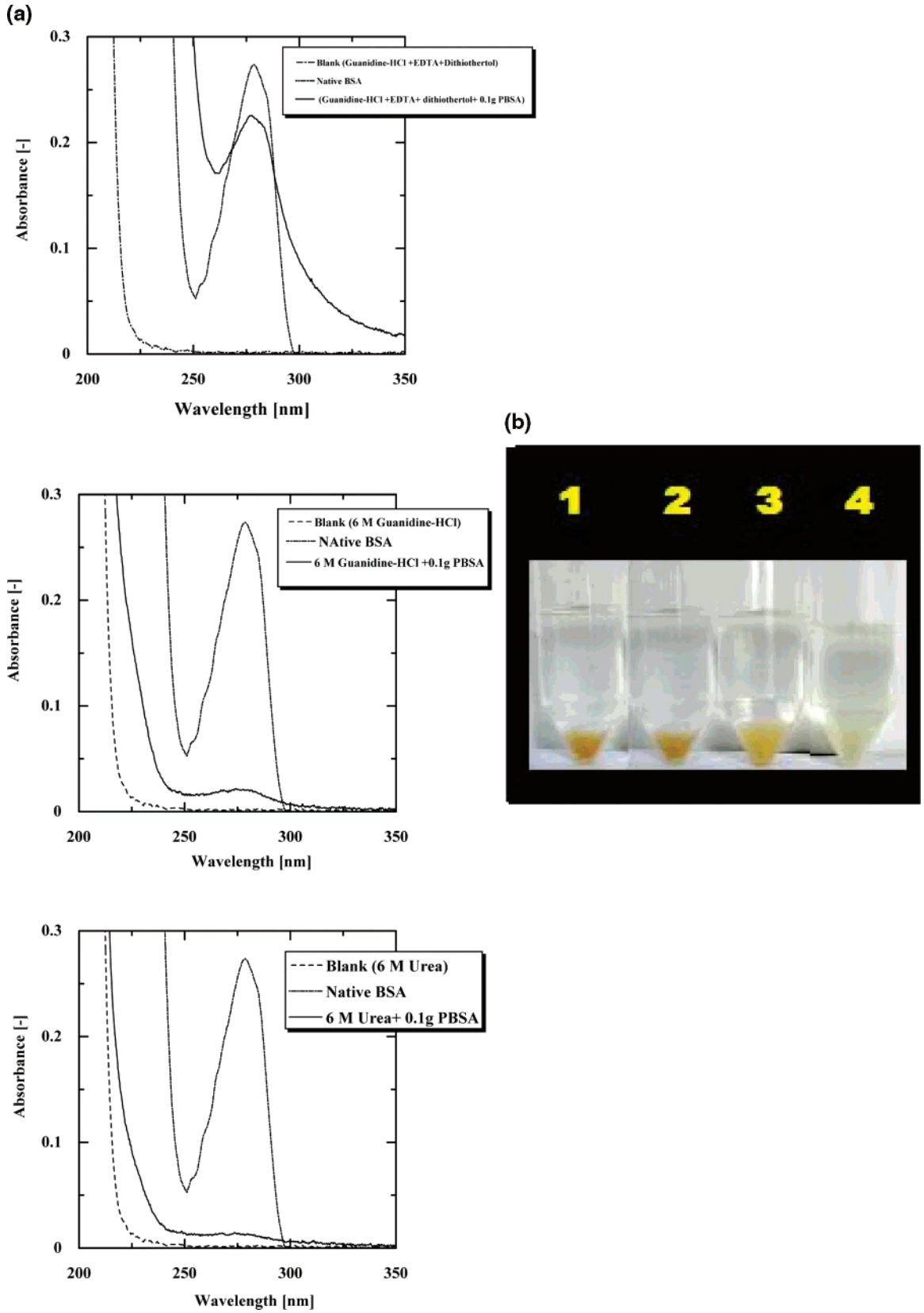

Figure 6. (a) UV spectra of the supernatant of different PBSA-containing solutions compared with their blanks. (b) Photograph of different solutions containing PBSA powdered after incubation at 298 K for 1 day.

These results revealed that the BSA molecules aggregated and grew in size (leading to the water-insolubility) in a polymerization fashion by being under the subcritical conditions. Finally, these aggregates resulted in a strong polymer matrix, which was stabilized by strong bonds.

To explore the bond involved in the aggregation and polymerization of the BSA under the sub-CW condition, we followed the same strategy adapted by Robert and others (*21*). The solubility of the PBSA in different denaturants was measured and compared. Table 1 shows the solubility results

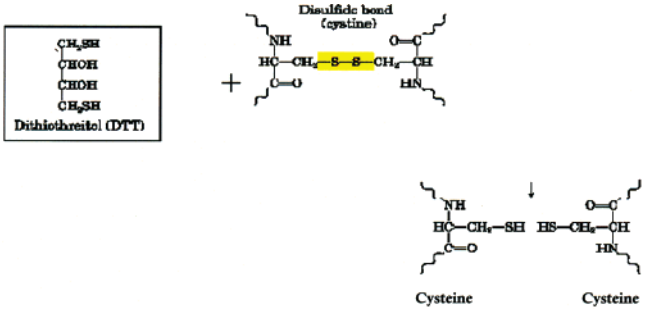

Figure 7. Reaction scheme of the breaking down of the disulfide bond reaction.

of the PBSA in various denaturant solutions, and Figure 6 shows the UV spectrum of the supernatant of different PBSA-containing solutions compared with their blanks (solution without PBSA). The results showed that strong denaturants such as 6 M urea and 6 M guanidine hydrochloride were unable to completely dissolve the PBSA molecules; only 5% and 7% of the PBSA molecules were dissolved, respectively. Actually, these denaturants are in the category of chaotropic agents (low-molecular-weight ionic compounds that enhance the solubility of hydrophobic compound in water by favoring the transfer of polar groups to water). Using such compounds at high concentrations (as in our case) will bring into solution both proteins or protein aggregates that have hydrogen bonds and hydrophobic interactions hindering their water solubility. These compounds are able to disrupt hydrogen bonds and hydrophobic interactions both between and within proteins and water. This in turn leads to disruption of the secondary protein structure and prevents aggregation. In fact, the hydrophobic attractions are most significant among the weak forces contributing to the solubility of the proteins in aqueous media. This is because van der Waals attractions between apolar groups are weak and hydrogen bonds of the C═O···H−N and C═O···H−O types are thermodynamically unstable if not protected from water (*22*). Adding such chaotropic agents to the PBSA-containing solution resulted in dissolution of a very small part of the PBSA. Such a result suggested that the hydrophobic interactions or other weak bonds do not represent the main interaction force holding the PBSA molecules together. This result leads to two important conclusions. First, the synthesis of the PBSA involved strong covalent bond interaction, specifically, disulfide bonds. Second, the reaction mechanism is not just an aggregation process but is extended to a polymerization stage.

The evidence of these speculations is strengthened by the fact that when the denaturant solutions contained a thiol reagent (0.2 M DTT and 10 mM EDAT to prevent its auto oxidation), more than 83% of the PBSA molecules was dissolved. These results indicate that the covalent linkages among PBSA molecules are mainly disulfide bonds, which are reduced when DTT is added. Figure 7 shows the scheme of the breaking mechanism of the disulfide bond of the PBSA formation by the DTT.

To investigate the role of the sub-CW in the intermolecular interaction, we had to gain more insight into the reaction environment. It is well understood that the sub-CW condition involves a unique combination temperature−pressure environment, both affecting the protein denaturation and aggregation. Generally, the chemical interactions that stabilize the native conformation of protein include the strong disulfide bonds and the weak noncovalent interactions such as hydrogen bonds, hydrophobic, ionic, and van der Waals interactions. Although all of these bonds are holding the protein molecules together, the overall stability of proteins is considerably low (*23*). Under high-temperature conditions, proteins denature. The mechanism of temperature-induced denaturation is highly complex and involves primarily destabilization of the major noncovalent interactions. Such interactions are exothermic in nature. Therefore, they are destabilized at high temperatures and stabilized at low temperatures. BSA was reported to pass through two structural stages when heat-treated. The first stage is reversible, whereas the second stage is irreversible. Heating up to 65 °C (under atmospheric pressure) can be regarded as the first stage, with subsequent heating above that as the second stage (*24*). Parallel to the structure deformation, BSA on heating formed soluble aggregates of polymerized molecules through disulfide and noncovalent bonds. The formation of such soluble aggregates and subsequent polymerization resulted in the formation of a rigid gel network (*25*, *26*).

Another important thermodynamic variable that affects denaturation of proteins is the hydrostatic pressure. Unlike temperature-induced denaturation, which usually occurs in the range of 313−353 K at 1 MPa, pressure-induced denaturation can occur at 298 K if the pressure is sufficiently great. Most proteins undergo pressure-induced denaturation in the range of 100−1200 MPa. The most basic concept to interpret the effects of pressure on chemical reactions is the principle of Le Chatelier, that is, pressure enhances chemical processes that result in volume decreases and diminishes that result in volume increases. Both ionization in aqueous system and disruption of hydrophobic interactions are accompanied by a decrease in volume. The main resources of such volume decreases come from either increase in solvent (water in the case of sub-CW reactions) exposure to amino acids side chains and peptide bonds or the diffusion of water into the cavities located in the hydrophobic core, respectively (*27*). Accordingly, the main targets of pressure on proteins are the electrostatic and hydrophobic interactions that maintain the higher structure of protein. On the contrary, the breakage of hydrogen bond sand covalent bonds results in volume expansion, and in turn it is restricted by the high pressure. It is important to note that high molecular weight aggregates are formed after pressure-induced unfolding of proteins and stabilized by intermolecular disulfide bonds. Such bonds are formed either by SH/S−S interchange reactions or by SH oxidation reactions (*28*−*30*). A fundamental difference between pressure and temperature induced protein denaturation is that no change in the covalent bonding has been observed in the pressure induced protein denaturation (*31*). Moreover, the pressure-denatured proteins are relatively compact and retain elements of secondary structure, whereas the heat-denatured proteins have the extended, nearly random coil configurations (*32*).

On the basis of the above discussion, it could be clearly realized that the sub-CW treatment with both high temperature and pressure provides a unique environment for the BSA molecules to produce a very stable polymer with highly ordered plastic configurations.

According to the above results and discussions, we can draw a mechanism for the synthesis process as following. First, at the early stage of the reaction, most of the energy is absorbed by the water molecules as a latent heat of vaporization. Both heat and generated vapor pressure at a considerably high temperature are responsible for the breaking down of both hydrophobic and electrostatic interactions without affecting the covalent and disulfide bonds inside the BSA molecules themselves and in turn initiating the aggregation step. Second, as shown in Figure 8, the BSA molecule contains eight cysteine residues and one free thiol of a cysteine residue. This free

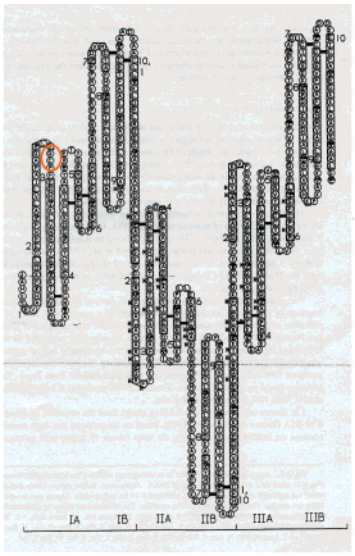

(a) Domains of the BSA molecule. The circle identifies the position of cysteine

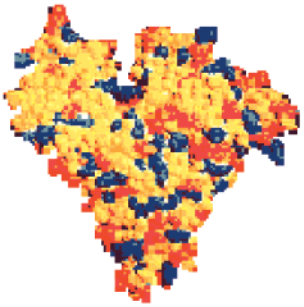

(b) Space filling model of a BSA molecule with basic residues colored in blue, acidic residues in red, and neutral ones in yellow

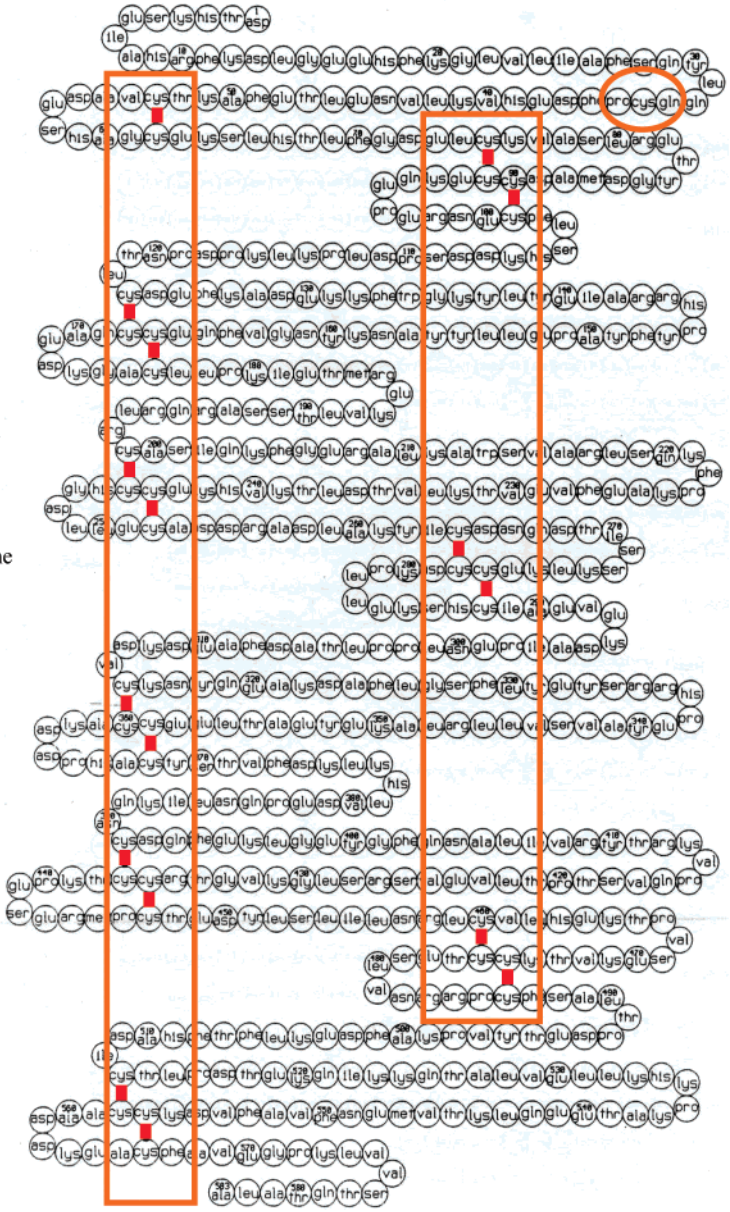

(c) Amino acid sequence of the BSA. The circle identifies the position of cysteine

Figure 8. (a) Space-filling model of BSA and (b) the disulfide bonds that hold the loops of BSA molecule. [Reproduced from Peters, R. Jr.; *All About Albumin*; Academic Press: New York, 1999]

cysteine is assumed to be responsible for forming a disulfide bond with another BSA molecule. The reaction mechanism could be viewed as a chain reaction based on the fact that the ionized thiol of one BSA molecule carries out a nucleophilic attack on a disulfide linkage of another BSA molecule. Consecutively, this reaction results in the formation of a new intermolecular S−S bond with release of a new free ionized thiol that in turn is capable of attacking another S−S bond of another BSA molecule. Thus, such interaction mechanism leads to propagation of the covalent polymerization processes. Actually, such a mechanism is supported by the SEM images, which showed a stepwise molecular propagation.

Reaction Kinetics. Prior to the kinetic study, the temperature profiles inside the reactor at different temperatures in the range of 473−523 K were measured and are shown in Figure 9. The experimental data was fitted with the heating and cooling equations obtained in our previous work (*18*). Using a nonlinear regression method, the heating and cooling rate constants, P_h and P_c, at different temperatures were calculated and are listed in Table 2. These parameters were used later in the kinetic models.

It is very important to note that the results shown in Figure 2 and explained above revealed that the reaction proceeded even at a very short time (less than 3 s even). Actually, we had great doubt about these results; how could the reaction proceed after only 2 s, when the temperature inside the reactor did not exceed 303 K at all tested temperatures? So, we repeated this experiment many times and found that the PBSA is formed even at 2 s reaction time. However, to solve this dilemma, we performed another experiment by heating the BSA solution under atmospheric pressure and followed the initiation of the aggregation process. Figure 10 shows test tubes containing the reaction

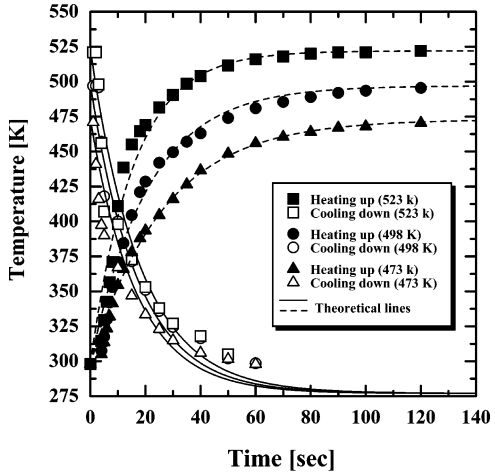

Figure 9. Temperature profile inside the tube batch reactor under the sub-CW conditions at different salt bath temperatures.

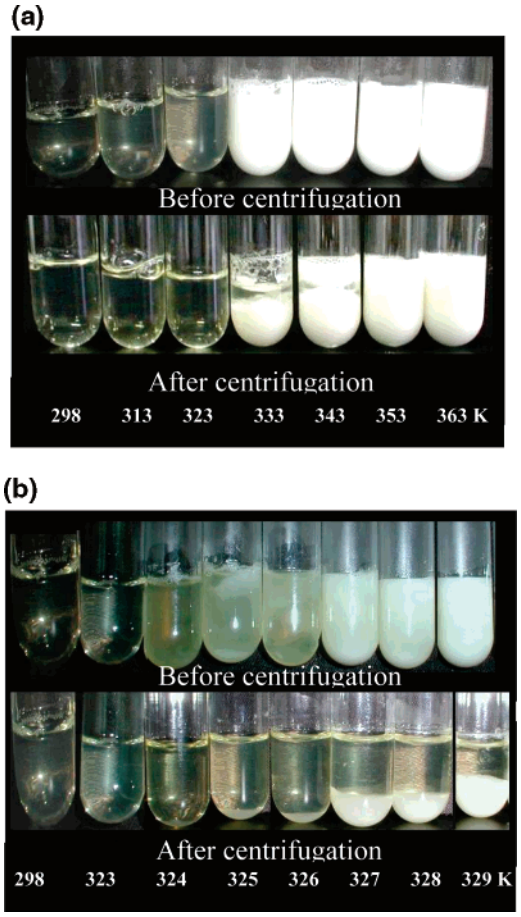

Figure 10. Photographs of the BSA solution before and after centrifugation at different temperatures (heating rate of 1 K/min) under atmospheric pressure.

media after heating at different temperatures in the range of 298−363 K and a varying heating time of 0−13 min (based on a heating rate of 5 K/min) before and after centrifugation (Figure 10a**)**. The results showed that the aggregation process initiated in the range of 323−333 K. Thus, we repeated the experiment again by restricting our observation in that range by taking samples each 1 K. The results shown in Figure 10b revealed that the aggregation step started at 324 K. Accordingly, the only accepted explanation for the reason of PBSA formation under

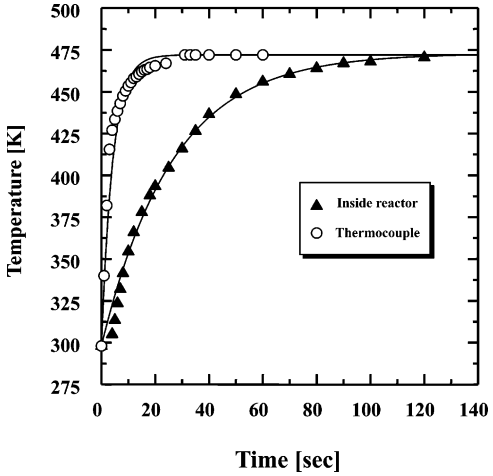

Figure 11. Temperature profile inside the tube batch reactor under the sub-CW conditions compared to the temperature profile of the thermocouple.

Table 2. Heating and Cooling Constants of the Batch Reactor Used at Different Salt Bath Temperatures

parameters	473 K	498 K	523 K
P_h	0.042	0.055	0.064
P_c	0.060	0.058	0.055

the sub-CW condition at such low inside reactor temperature is that the PBSA is formed at the inside wall of the reactor, where the temperature is higher than that in the middle of the reactor. To prove that, we measured the temperature of the reactor wall by dipping the thermocouple directly into the salt bath (neglecting the heat losses across the reactor stainless steel wall), and the obtained results were compared with that obtained by measuring the inside of the reactor under the sub-CW at 473 K as shown in Figure 11. The results showed that at 1 s, the temperature inside the reactor was less than 303 K, whereas at the wall of the reactor the temperature was 340 K. According to these results we should take into consideration that any experimental data collected in the range of 298−340 K under the tested condition would be due to the wall effect and not due to the sub-CW reaction. Such a result leads to the fact that the batch reactor used in this study failed in collecting the data in that range.

To follow the reaction kinetic, the time course of the PBSA synthesis reaction was followed by measuring the protein concentration of the liquid phase of the reaction product at different temperatures. Figure 12a−c shows the time course of the PBSA formation at three different temperatures 473, 498, and 523 K, respectively. The theoretical lines in the figures were calculated on the basis of the kinetic model developed in our previous work (*18*) and briefly explained in the theory section of this work. According to the strategy developed in our previous work, the first step was the evaluation of initial values of activation energy (E) and pre-exponential factor (A) required to start the trial and error routine. Theses values were evaluated assuming that the reaction is taking place under a steady-state condition and follows a first-order kinetic. So, the reaction rate constants at different temperatures were evaluated from the slope of the straight line resulting from the plot of the $-\ln[1 - x]$ (where x represents the conversion of the BSA) against the residence time. The E and A values were calculated on the basis of two different assumptions: first, by assuming the reaction is taking place at the salt bath temperature (the steady-state temperature), and second, by assuming that the reaction is taking

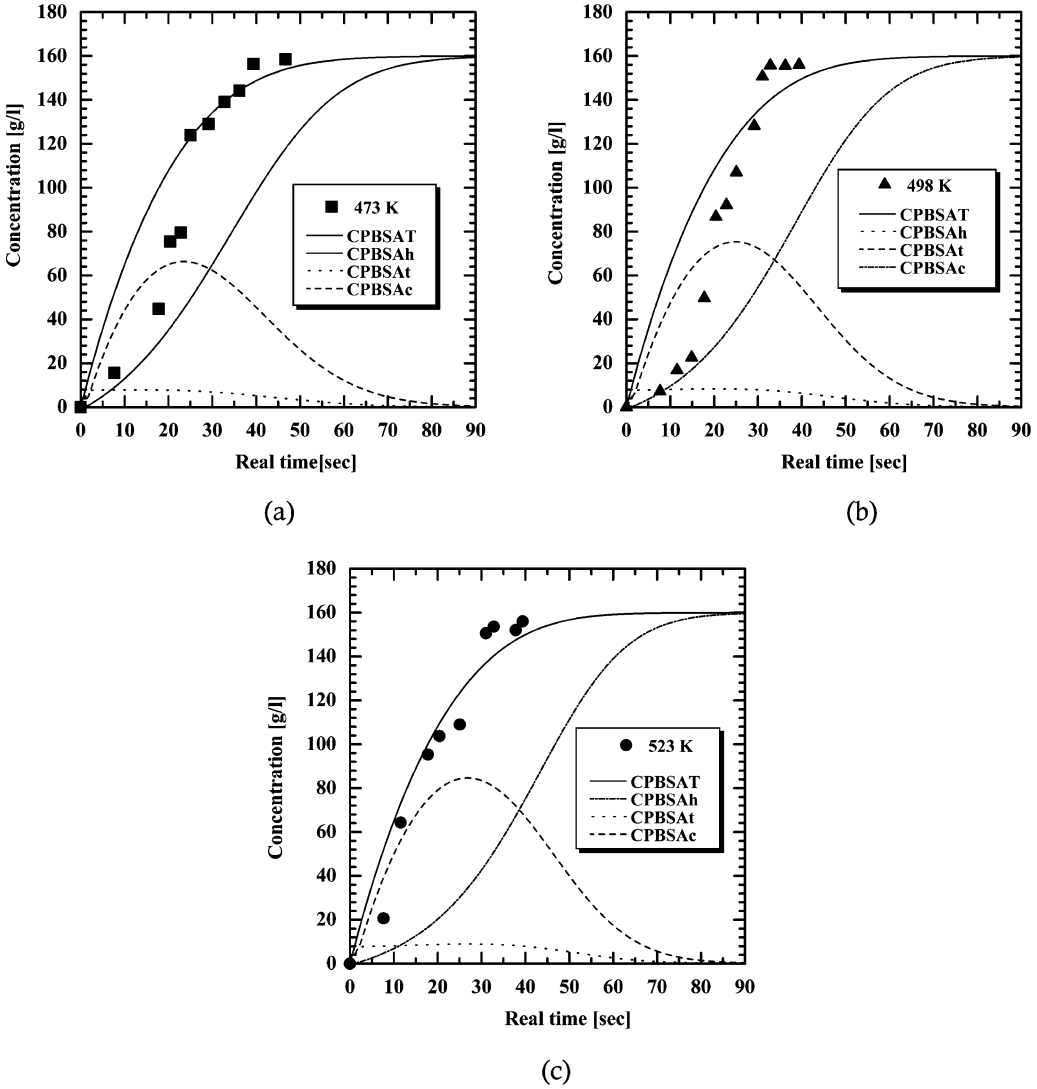

Figure 12. Time course of PBSA formation under the sub-CW conditions at different temperatures. The marked areas represent the time needed for the reaction mixture to reach 324 K.

Table 3. Kinetic Parameters of the PBSA Synthesis Reaction

reaction rate constant [s^{-1}]			activation energy [kJ/mol]			frequency factor [s^{-1}]		
k_{473}	k_{498}	k_{523}	$E_{\text{salt bath}}{}^{a}$	$E_{\text{average}}{}^{b}$	$E_{\text{model}}{}^{c}$	$A_{\text{salt bath}}{}^{a}$	$A_{\text{average}}{}^{b}$	$A_{\text{model}}{}^{c}$
0.151	0.153	0.226	17.6	10.6	7.2	12.7	5.2	0.9

[a] Calculated considering the reaction takes place at the steady-state bath temperature. [b] Calculated considering the reaction takes place at the average temperature reached during the cures of the reaction. [c] Calculated considering the reaction takes place under unsteady state.

place at the average temperature value reached during the period of the reaction time. The values of the calculated *E* and *A* values under the two different assumptions are listed in Table 3. Starting from these values, a trial and error routine was initiated using the computer program developed in our previous work to find out the best values for E and A that could fit the experimental data. The best values for *E* and *A* were found to be 7.2 kJ/mol and 0.9 s^{-1}, respectively. As shown in Figure 12 the theoretical lines obtained using these values are in considerably good agreement with the experimental data except in the very early stage of the reaction (due to the wall effect explained above). The obtained *E* and *A* values were small compared to those obtained considering the reaction takes place under either steady-state salt bath temperature or the average temperature reach during the course of the reaction time. The low *E* value signifies that large numbers of collisions of BSA molecules had enough energy to form the activated complex, which finally led to the synthesis of the product PBSA. As a result, the reaction was so fast that it took place in a very short time. On the other hand, such very low *A* value signifies that the frequency of the collision is very low and the reaction was very close to being independent of the activation energy (note that *A* is close to the reaction rate constants measured under the assumption that the reaction is following first-order kinetic under a steady-state temperature). These obtained results may imply a certain role of diffusion in the reaction mechanism. Since such low values of *E* and *A* indicate that the reactions between the BSA molecules occur at nearly every collision, therefore the reaction may be considered to proceed near to the diffusion limit. Such mechanism could be viewed that BSA forms an immobile seed and another BSA molecule is then launched from a random position far away and is allowed to diffuse. If it touches the

BSA-seed, it is immobilized instantly by the act of different interaction forces (as described above) and becomes a part of the aggregate. Then this process is repeated with a similar BSA molecule one-by-one, and each of them stops upon hitting the cluster. After a few hundred particles, a cluster with intricate branch structures results and the cluster grows in size (as shown previously in the SEM image), and then for another new BSA molecule it will build up by time a diffusion barrier and the process will run under a diffusion control mechanism.

Conclusions

The synthesis of PBSA involves a two-step mechanism. First, at the early stage of the reaction, both high pressure and temperature lead to the breaking down of both hydrophobic and electrostatic interactions without affecting the covalent and disulfide bonds. Second, the free cysteine is assumed to be responsible for forming a disulfide bond with another BSA molecules and the reaction mechanism could be viewed as a chain reaction. The obtained E and A values signify that the reaction is relatively temperature-insensitive and furthermore it may be restricted to some extend to a diffusion limitation.

References and Notes

(1) Krammer, P.; Vogel H. Hydrolysis of esters in subcritical and supercritical water. *J. Supercrit. Fluids* **2000**, *16*, 189−206.

(2) Tromp, R. H.; Postorino, P.; Neilson, G. W.; Ricci, M. A.; Soper, A. K. Neutron diffraction studies of H_2O/D_2O at supercritical temperatures: a direct determination of gHH(r), gOH(r) and gOO-(r). *Chem. Phys*. **1994**, *101*, 6210−6214.

(3) Ohtaki, H.; Radnai, T.; Yamaguchi, T. Structure of water under thesubcritical and supercritical conditions studied by means of solution X-ray diffraction. *Chem. Soc. Rev.* **1997**, 41−51.

(4) Deshpande, G. V.; Holder, G. D.; Bishop, A. A.; Gopal, J.; Wender, I. Extraction of coal using supercritical water. *Fuel* **1984**, *63*, 956−960.

(5) Kershaw, J. R. Supercritical fluids in coal processing. *Environ. Sci. Technol.* **1993**, *27*, 806−809.

(6) Daimon, H.; Kang, K.; Sato, N.; Fuje, K. Development of marine waste recycling technologies using sub- and supercritical water. *Chem. Eng. Jpn.* **2001**, *34*, 1091−1096.

(7) Modell, M. *Standard Handbook of Hazardous Waste Treatment and Disposal*; Freeman, H. M., Ed.; McGraw Hill: New York, 1989; Sec. 8.11.

(8) Goto, M.; Nada, T.; Kodama, A.; Hirose, T. Kinetic analysis for destruction of municipal sewage sludge and alcohol distillery wastewater by subcritical water oxidation. *Ind. Eng. Chem. Res*. **1999**, *38*, 1863−1865.

(9) Yoshida, H.; Terashima, M.; Takahashi, Y. Production of organic acids and amino acids from fish meat bysubcritical water hydrolysis. *Biotechnol. Prog.* **1999**, *15*, 1090−1094.

(10) Yoshida, H.; Atarashi, M.; Shigeta, T. Conversion of entrails of fish waste to valuable resources by subcritical water hydrolysis. In *Proceeding of Joint Sixth International Symposium on Hydrothermal Reactions and Fourth International Conference on Solvo-Thermal Reactions*; July 2000, Kochi, Japan; pp 122−125.

(11) Yoshida, H.; Takahashi, Y.; Terashima, M. A simplified reaction model for production of oil, amino acids and organic acids from fish meat by hydrolysis under subcritical and supercritical conditions. *J. Chem. Eng. Jpn.* **2003**, *36* (4), 441−448.

(12) Yoshida, H.; Tavakoli, O. Subcritical water hydrolysis treatment of squid waste entrails and production of organic acid, amino acid, and fatty acids. *J. Chem. Eng. Jpn*. **2004**, *37* (2), 253−260.

(13) Yoshida, H.; Nakahashi, T. Production of useful substances from meat and bone meal by subcritical water hydrolysis. *Proceeding of the 10th APCChE Congress* **2004**, 3P-03-025.

(14) Tavakoli, O.; Yoshida, H. Effective recovery of harmful metal ions from squid wastes using subcritical and supercritical water treatment. *Environ. Sci. Technol.* **2005**, *39* (7), 2357−2363.

(15) Yoshida, H.; Katayama, Y. Production of useful substances from wood wastes by subcritical water hydrolysis. *Preceding of 10th the APCChE Congress* **2004**, 3P-03−025.

(16) Abdelmoez, W.; Yoshida, H. An overview of the applications of the subcritical water hydrolysis technology in waste reuse, recycle, and treatment. *Proceedings of El-Minia International Conference, Towards a Safe and Clean Environment, TSCE'05*; El-Minia, Egypt 2005a, 15−17 April; E3−4.

(17) Abdelmoez, W.; Yoshida, H. Synthesis of a novel protein-based biodegradable plastic from the BSA using the sub-critical water technology. *AIChE J*. **2006**, *52* (7), 2607.

(18) Abdelmoez, W.; Yoshida, H. Modeling and simulation of fast reactions in batch reactors under sub-critical water condition. *AIChE J*. **2006**, *52* (10)

(19) Laemmli, U. K. Cleavage of structural proteins during the assembly of the head of bacteriophage T4. *Nature* **1970** Aug 15, *227* (5259), 680−685.

(20) Weber, K.; Osborn, M. The reliability of molecular weight determinations by dodecyl sulfate-polyacrylamide gel electrophoresis. *J. Biol. Chem.* **1969** Aug 25, *244* (16), 4406−4412.

(21) Lui, W. R.; Langer, R.; Klibanov, A. M. Moisture-induced aggregation of lyophilized proteins in solid state. *Biotechnol. Bioeng.* **1992**, *37*, 177−184.

(22) Hatef, Y.; Hanstein, W. G. Solubilization of particulate proteins and nonelectrolytes by chaotropic agents. *Biochem. J*. **1969**, *62*, 1129−1136.

(23) Lehninger, A. L.; Nelson, D. L.; Cox, M. M. *Principles of Biochemistry*; Worth Publishers, Inc.: New York 1993.

(24) Kuznetsow, A. N.; Ebert, B. G.; Lassmann, A. B. Shapiro adsorption of small molecules to bovine serum albumin studied by the spin-probe method. *Biochim. Biophys. Acta* **1975**, *379*, 139−146.

(25) Nakamura, T.; Utsumi, S.; Mori, T. Interaction during heat induced gelation in a mixed system of soybean 7S and 11S globulins. *Agric. Biol. Chem.* **1986**, *50*, 2429−2435.

(26) Kitabatake, N.; Tani, Y.; Doi, E. Rheological properties of heat induced ovalbumin gels prepared by two-step and one-step heating methods. *J. Food Sci*. **1989**, *54*, 1632−1638.

(27) Hayashi, R. Utilization of pressure in addition to temperature in food science and technology. In *High Pressure and Biotechnology*; Balny, C., Hayashi, R., Heremans, K., Masson, P., Eds.; John Libbey Eurotext: Montrouge, France, 1992; pp 185−192.

(28) Funtenberger, S.; Dumay, E.; Cheftel, J. C. Pressure-induced aggregation of β-lactoglobulin in pH 7.0 buffers. *Lebensm.-Wiss. Technol.* **1995**, *28*, 410−418.

(29) Van Camp, J.; Feys, G.; Huyghebaert, A. High pressure-induced gel formation of haemoglobin and whey proteins at elevated temperatures. *Lebensm.-Wiss. Technol*. **1996**, *29*, 49−57.

(30) Messens, W.; Van Camp, J.; Huyghebaert, A. The use of high pressure to modify the functionality of food proteins. *Trends Food Sci. Technol.* **1997**, *8*, 107−112.

(31) Cheftel, J. C. Effect of high hydrostatic pressure on food constituents: an overview. In *High Pressure and Biotechnology*; Balny, C., Hayashi, R., Heremans, K., Masson, P., Eds.; John Libbey Eurotext: Montrouge, France, 1992; pp 195−203.

(32) Ghosh, T.; Garcia, A. E., Garde, S. Molecular dynamics simulations of pressure effects on hydrophobic interactions. *J. Am. Chem. Soc*. **2001**, *123*, 10997−11003.

Received July 29, 2007. Accepted November 19, 2007.

BP0702572